Annals of Nuclear Medicine Vol. 15, No. 3, 191–198, 2001

Binding rate constant of Tc-99m DTPA galactosyl human serum albumin measured by quantitative dynamic SPECT —Clinical evaluation as a total and regional liver function test—

Koichiro YAMAKADO,* Kaname MATSUMURA,* Yoshiyuki TAKASHIBA,* Atsuhiro NAKATSUKA,* Tokio KITANO,* Takashi ICHIHARA,*** Hisato MAEDA,**** Kojiro TAKASE** and Kan TAKEDA*

*Department of Radiology, **First Department of Internal Medicine, Mie University School of Medicine
***Toshiba Medical Engineering Laboratory
****Fujita Health University School of Health Science

To evaluate the clinical utility of a new method with dynamic single photon emission computed tomography (SPECT) and scatter and attenuation compensation to estimate both total and regional liver function quantitatively. Five controls, 20 patients with chronic liver disease, and 2 patients with Budd-Chiari syndrome were studied. Dynamic liver SPECT data were acquired during 20 minutes after injection of Technetium (Tc)-99m diethylenetriaminepentaacetic acid (DTPA) galactosyl human serum albumin (GSA) with scatter and attenuation compensation. The binding rate constant of Tc-99m GSA (K_u) was derived quantitatively from the Patlak plot based on kinetic models for GSA receptor binding. The mean K_u was obtained by dividing the K_u value (total K_u) by the liver volume. Both total and mean K_u were significantly lower in patients with chronic liver disease than in controls (302 ± 112 vs. 523 ± 78 ml/min; $p < 0.001$, 0.26 ± 0.11 vs. 0.43 ± 0.03 ml/min/cm^3; $p < 0.001$). In the patient group, both total and mean K_u were significantly correlated with the results of conventional liver function tests and the histological severity of chronic liver disease. In 2 patients with Budd-Chiari syndrome, the mean K_u was lower in the right lobe, where the hepatic veins were occluded, than in the left lobe, where draining veins were patent. In conclusion, this method is a reliable diagnostic technique for estimating total and regional liver function.

Key words: dynamic SPECT, Tc-99m DTPA galactosyl human serum albumin, liver function test, chronic liver disease, Budd-Chiari syndrome

INTRODUCTION

DIETHYLENETRIAMINEPENTAACETIC ACID (DTPA) galactosyl human serum albumin (GSA) is an analog ligand to the asialoglycoprotein (ASGP) receptor, which resides on the plasma membrane of mammalian hepatocytes and is responsible for the metabolism of serum glycoproteins.[1–3] Technetium (Tc)-99m GSA scintigraphy can help to probe ASGP receptor biochemistry and reflect the liver function.[4,5] Vera et al. advocated the kinetic model for Tc-99m-galactosyl-neoglycoalbumin (NGA) receptor binding.[6] This kinetic model is considered to be applied to Tc-99m GSA kinetics because NGA and GSA are almost the same pharmaceutical.[7] The fundamental components that govern the rate of the receptor-binding process are the receptor and ligand concentrations, and the forward and reverse binding rate constants.[8] Tc-99m GSA dynamic data provide valuable information *in vivo* regarding the receptor population density.[9,10] Some investigators have reported the utility of Tc-99m GSA liver scintigraphy in evaluating total liver function.[11–13] These studies were performed by acquiring Tc-99m GSA dynamic data by means of planar images. Recently, Hwang has reported

Received April 24, 2000, revision accepted December 21, 2000.

For reprint contact: Koichiro Yamakado, M.D., Department of Radiology, Mie University School of Medicine, 2–174, Edobashi, Tsu, Mie 514–8507, JAPAN.
E-mail: yama@clin.medic.mie-u.ac.jp.

the clinical usefulness of Tc-99m GSA dynamic single photon emission computed tomography (SPECT) with Patlak plot to estimate hepatic functional reserve.[9] On the other hand, we have developed and reported preliminary results for a new method for measuring the binding rate constant (K_u) with dynamic SPECT from the Patlak plot.[14–16] The K_u is considered to represent the maximum removal rate of Tc-99m GSA that reflects receptor population density.[17] Our method seems to have some advantages in evaluating liver function for the following reasons: a) since the time-activity curve of the liver can be acquired with scatter and attenuation compensation, the parameters obtained permit the quantitative evaluation of liver functions, b) both total and regional liver function can be evaluated quantitatively. In the present study, we evaluated the clinical usefulness of our method in the evaluation of liver function.

MATERIALS AND METHODS

Subjects

Tc-99m GSA studies were performed in 5 volunteers with normal livers, 20 patients with chronic liver disease and 2 patients with Budd-Chiari syndrome. The control group consisted of 5 men with a mean age of 36 years (range, 24–60 years). All control subjects had normal liver function tests and had no history of liver disease. The chronic liver disease group consisted of 5 women and 15 men with a mean age of 54 years (range, 27–75 years). The diagnosis of chronic liver disease was histologically confirmed by laparoscopic biopsy in 13 patients. In the other 7 patients, the diagnosis was based on ultrasonographic findings, laboratory tests, and evidence of viral infection (hepatitis C viral antibody positive: 18 patients, hepatitis B viral antigen positive: 2 patients). Two patients with Budd-Chiari syndrome were a 38-year-old woman and a 55-year-old man. The inferior vena cava and all hepatic veins were occluded before percutaneous transcatheter angioplasty (PTA) in both patients. PTA was performed, and both the inferior vena cava and left hepatic vein was recanalized, but, the right and middle hepatic veins were still occluded in both patients when Tc-99m GSA studies were done.

Tc-99m GSA study

Before injection of Tc-99m GSA, a tomographic transmission study was done to obtain the attenuation coefficient map: 60 images were acquired over a 360-degree orbit over 20 minutes in continuous scanning mode (four rotations at 5 minutes/rotation). Attenuation and scatter compensation was done with the flood source method for transmission computed tomography (TCT)[14,18–21] with a dual-head SPECT system (GCA-7200A, Toshiba, Nasu, Japan). The projection data were subjected to Butterworth filter processing before reconstruction. The TCT images were reconstructed by filtered backprojection with a Shepp & Logan filter and a slice thickness of 8.6 mm (1 pixel).

Patients received 148 MBq (4 mCi) of Tc-99m GSA by intravenous injection. Forty sequential 30-second SPECT data were acquired in the first 20 minutes after the injection. For triple energy window (TEW) scatter correction,[18] SPECT data and scatter rejection data were acquired with 141 ± 14 keV and 117.2–127 keV energy windows, respectively. Projection data were acquired with an acquisition time of 1 sec per view (30 sec per scan).

Ten minutes after intravenous Tc-99m GSA injection, a blood sample was collected from a contralateral antecubital vein. The whole blood radioactivity was measured with a well-type scintillation counter (ATC-301, Aloka, Tokyo, Japan). The reference sample was washed and diluted in 1,000 m*l* of water, and the radioactivity of 1 m*l* of the diluted reference tracer was measured. Based on the radioactivity of the reference, the blood radioactivity was measured in units of μCi/m*l*. SPECT images were reconstructed with a Shepp & Logan filter. The projection data were subjected to Butterworth filter processing before reconstruction. Attenuation compensation was performed with a 2-iteration Chang algorithm that was modified to incorporate a measured nonuniform attenuation map.[21] The SPECT value (count) was converted to activity with the cross-calibration factor,[14] pixel length, slice thickness, and acquisition time. Measured activity (μCi) = Cross calibration factor (μCi·sec/count)·SPECT value (count)/acquisition time (sec).

A region of interest (ROI) was specified over the heart on a summed image of a few selected 1-minute SPECT slices. The time-activity curve (TAC) of the heart was generated by plotting the counts in the ROI over the serial summed images against the respective mid-points in time during the serial SPECT data collection periods. The cardiac TAC [Hspect(t)] was approximated by the least-squares fitting method on the basis of the biexponential function with data from 2 to 20 minutes after injection.

An ROI for the entire liver was specified over a series of the summed images of the respective slices covering the liver by cutting off a fixed count. The SPECT images were rearranged to create serial summed liver SPECT images, in each of which all slices covering the liver were summed. The serial total liver counts were then measured over 20 minutes. The TAC of the entire liver [L(t)] was generated by plotting the total liver counts against the midpoints in time during the respective SPECT data collection periods. Five-minute SPECT data, the midpoint in time of which was a 15-minute injection, were merged from the serial SPECT data. In the 2 patients with Budd-Chiari syndrome, each ROI for the entire liver, right lobe and left lobe was specified referring to the CT images, and the same data analysis was performed for each ROI.

Data analysis

We calculated the K_u value for the total liver (total K_u)

with dynamic Tc-99m GSA SPECT as described below.[14] The cardiac TAC of Hspect(t) (μCi) can be converted to the radioactivity concentration in the blood H(t) (μCi/ml) as follows. The radioactivity concentration in venous blood obtained 10 minutes after tracer injection is expressed as H.[10] The 10-minute value is measured from the above-mentioned approximated cardiac TAC [Hspect (10)]:

$$H(t)\ (\mu Ci/ml) = \frac{Hspect(t)\ (\mu Ci) \times H(10)\ (\mu Ci/ml)}{Hspect(10)\ (\mu Ci)} \quad (1)$$

The K_u is obtained with equation (2):

$$L(t)/H(t) = K_u \int_0^t H(t)dt + V_h \quad (2)$$

where [L(t)] is the hepatic radioactivity concentration measured by SPECT, and V_h is the hepatic blood volume in a unit volume of the liver. The liver TAC of L(t) is expressed in units of [mCi]; H(t), the blood concentration curve is expressed in units of [mCi/ml]; and V_h, the hepatic blood pool volume, in units of [ml], so $V_hH(t)$ is in units of [mCi]. $\int_0^t H(t)dt$ is expressed in units of [mCi min/ml] and K_u in units of [ml/min], so $K_u \int_0^t H(t)dt$ is also in units of [mCi]. Using measured L(t) and H(t) data, L(t)/H(t) was plotted against $\int_0^t H(t)dt/H(t)$ and linear approximation was performed at points from 86 s to 400 s. K_u and V_h values were determined as the slope and intercept, respectively, by this linear approximation.

Volume measurement of the liver and calculation of mean K_u

To calculate the mean K_u, the volume of the whole liver was obtained. Volume measurement was performed with the CT system in 5 controls, 16 patients with chronic diseases and 2 patients with Budd-Chiari syndrome[22–24] because it was difficult to identify the edges of the liver on SPECT images in some patients with poor liver profiles (Fig. 3b). CT images were obtained covering the whole liver with a helical CT system (X-vigor, Toshiba, Nasu, Japan). Helical CT scans were acquired during a single breath hold.[25] Parameters for helical CT were 5–10 mm collimation and 5–10 mm/sec table sliding. Contiguous axial sections 5 or 10 mm thick were reconstructed from the volumetric data. The total liver area was measured by tracing on each CT image. The volume of the whole liver was then automatically calculated by multiplying each area by the slice thickness. In 2 patients with Budd-Chiari syndrome, the volumes of the right and left lobes were measured. The mean K_u value was calculated by dividing the total K_u value by the volume of the whole liver (ml/min/cm^3). The total and mean K_u values were calculated in the right and left lobes, respectively.

Liver functional imaging

The mean TAC of the liver L(t) was generated by plotting the liver counts for each pixel in the SPECT slice against the respective midpoint in time of the serial SPECT data. By the same data processing as mentioned above, the K_u values for each voxel were obtained and the respective distribution images corresponding to the original SPECT images were generated. This functional image displays the distribution of K_u per voxel (ml/min/voxel) values.

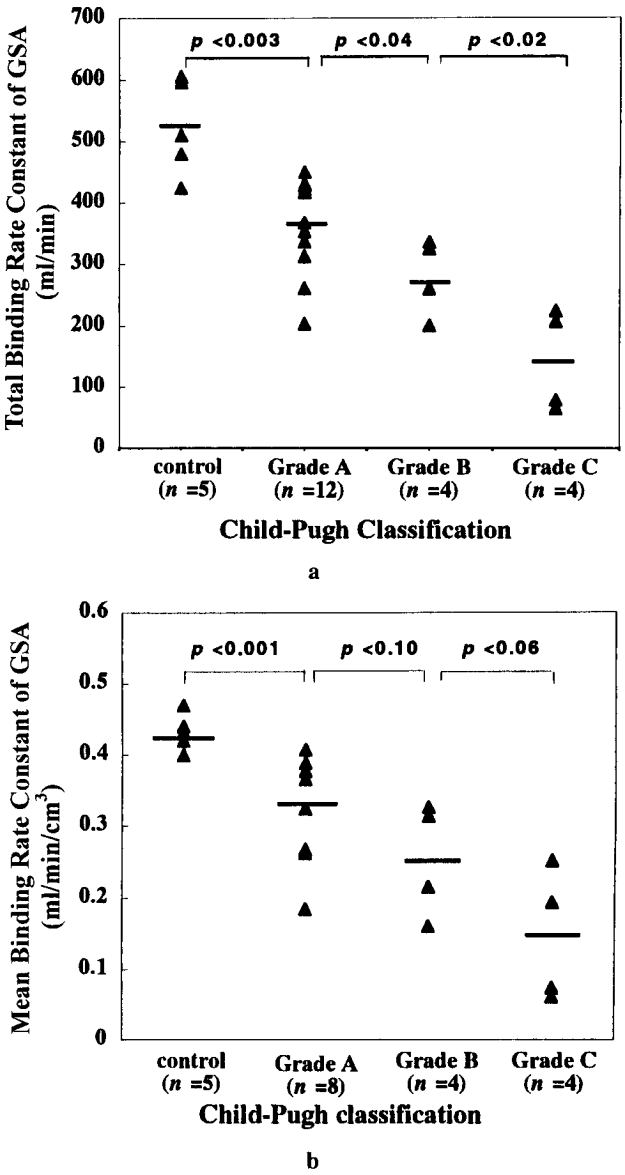

Fig. 1 Relationships between total (a) and mean (b) K_u and the severity of liver disease (Child-Pugh classification). Both values clearly reflect the severity of liver disease.

Assessment of clinical significance

The severity of chronic liver disease was classified into three groups, based on the Child-Pugh classification.[26] Twelve patients had grade A liver profiles, 4 patients had grade B liver profiles, and 4 patients had grade C liver profiles. The total and mean K_u values were evaluated in controls and in patients with various degrees of chronic liver disease.

Relationships between the total and mean K_u values and the following conventional liver function tests were

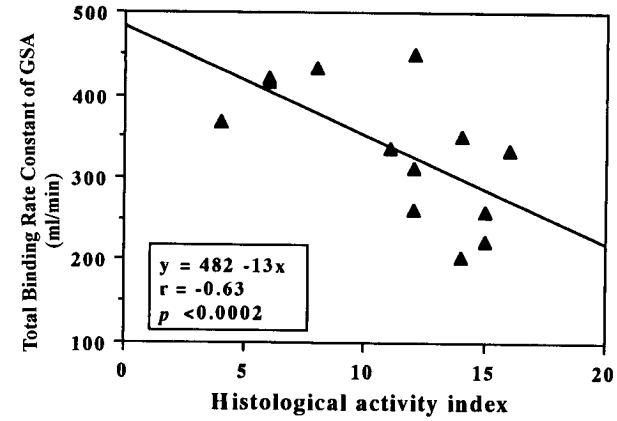

a

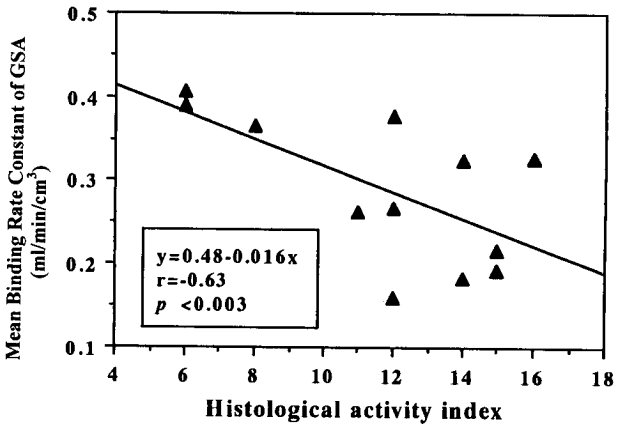

b

Fig. 2 Correlation of the total (a) and mean (b) K_u with histological severity (histological activity index) of chronic liver disease. Both values are significantly correlated with the histological severity.

evaluated: asparatate aminotransferase (AST) (IU), alanine aminotransferase (ALT) (IU), the serum albumin level (g/dl), serum bilirubin level (mg/dl), serum cholinesterase activity (ΔpH), prolongation of prothrombin time (%), normotest (%), and plasma retention rate for indocyanine green at 15 minutes (ICG R15) (%).

The total K_u value was evaluated and compared with the histological severity of chronic disease in 13 patients who underwent biopsy. The relationship between the mean K_u value and histological severity was also compared in 12 patients. Histological severity was assessed with the histological activity index score (HAI score).[27]

Statistical analysis

Data are expressed as the mean ± standard deviation. The total and mean K_u values in the controls and in patients with liver disease were compared statistically by Student's t test. Correlation of total and mean K_u values with each liver function test and the HAI score was analyzed by standard Pearson correlation analysis. A p value of less than 0.05 was considered statistically significant.

RESULTS

Correlation of total and mean K_u with conventional liver function tests

The total and mean K_u values according to the Child-Pugh classification are shown in Figure 1. Both values were lower in patients with chronic liver disease than in the controls. For the total K_u, the value in the controls was 523 ± 78 ml/min and that in patients with chronic liver disease was 302 ± 112 ml/min ($p < 0.001$). The mean K_u value in the controls was 0.43 ± 0.03 ml/min/cm^3 and that in patients with chronic liver disease was 0.26 ± 0.11 ml/min/cm^3 ($p < 0.001$). In patients with chronic liver disease, both total and mean K_u values clearly reflected the severity of the liver profile. The total K_u values according

Table 1 Correlation of total and regional effective hepatic blood flow with conventional liver function tests

Liver function tests	Total EHBF		Regional EHBF	
	Correlation coefficiency (r)	p value	Correlation coefficiency (r)	p value
Asparatate aminotransferase	0.564	< 0.0001	−0.461	0.073
Alanine aminotransferase	0.62	< 0.0001	−0.216	0.43
Albumin	−0.484	< 0.0001	−0.015	0.82
Bilirubin	−0.836	< 0.0001	−0.305	< 0.0001
Cholinesterase	−0.845	< 0.0001	−0.56	< 0.0001
Prothrombin time	0.127	0.062	0.341	< 0.0001
Normo test	0.951	< 0.0001	0.486	< 0.0001
ICG R15	−0.772	< 0.0001	−0.779	< 0.0005

ICG R15: plasma retension rate of indocyanine green at 15 minutes
EHBF: effective hepatic blood flow

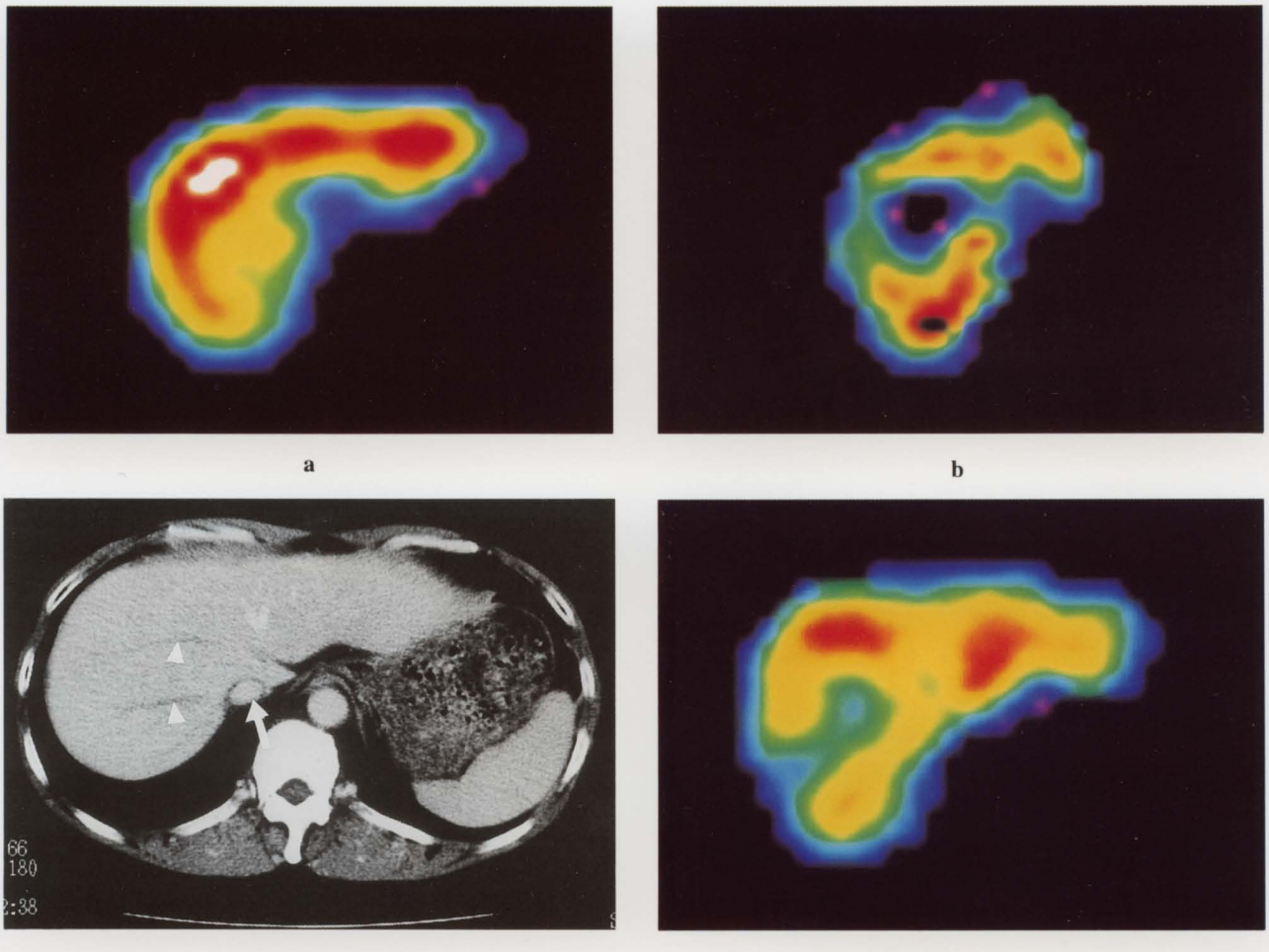

Fig. 3 a: Liver functional image of mean K_u in a control subject. The maximum K_u value per voxel is displayed as 0.55 ml/min/cm^3, and the minimum value as 0 ml/min/cm^3. The mean K_u is diffuse throughout the entire liver parenchyma. The total K_u is 479 ml/min and the mean K_u is 0.40 ml/min/cm^3 in this control subject. b: Functional image of mean K_u in a patient with a severe liver profile (Child-Pugh grade C). The maximum K_u value per voxel is displayed as 0.05 ml/min/cm^3, and the minimum value as 0 ml/min/cm^3. Atrophy of both the right and left lobes and hypertrophy of the caudate lobe are seen. The mean K_u is markedly decreased and its distribution is irregular compared with the controls. Note the increased mean K_u in the caudate lobe. The total K_u is 65 ml/min and the mean K_u is 0.06 ml/min/cm^3 in this patient. c and d: Computed tomography (c) and functional (d) image in a patient with Budd-Chiari syndrome. The inferior vena cava and left hepatic vein are patent after transcatheter angioplasty (arrows). The right and middle hepatic veins are still occluded (arrowheads) (c). The functional image shows hypertrophy of the left lobe and atrophy of the right lobe, and clearly demonstrates a lower mean K_u in the right lobe compared with the left lobe. The mean K_u is 0.31 ml/min/cm^3 in the right lobe and 0.44 ml/min/cm^3 in the left lobe, respectively, in this patient.

to Child-Pugh classification were as follows: Grade A (n = 12): 362 ± 75 ml/min, Grade B (n = 4): 280 ± 63 ml/min, and Grade C (n = 4): 144 ± 83 ml/min. The mean K_u values were as follows: Grade A (n = 8): 0.32 ± 0.08 ml/min/cm^3, Grade B (n = 4): 0.25 ± 0.08 ml/min/cm^3, and Grade C (n = 4): 0.15 ± 0.09 ml/min/cm^3. Correlations between total and mean K_u values and conventional liver function tests are shown in the Table 1. The total K_u value was significantly correlated with conventional liver function tests except for percent prothrombin time. The mean K_u value was significantly correlated with those except for AST, ALT and albumin.

Correlation of total and mean K_u with histological activity index

The results are shown in Figure 2. Both total and mean K_u values were significantly correlated with the histological severity of chronic liver disease (HAI score) (total K_u: $r = -0.63$, $p < 0.0002$, mean K_u; $r = -0.63$, $p < 0.003$).

Total and mean K_u in patients with Budd-Chiari syndrome

The total Ku values were lower in 2 patients with Budd-Chiari syndrome than in the controls (324 and 335 ml/min, respectively). A difference in the mean K_u value was seen between the right and left lobes in both patients. Although the mean K_u value was lower in the right lobe, it was similar to that in the control subjects in the left lobe. The mean K_u was 0.29 ml/min/cm^3 in the right lobe and 0.39 ml/min/cm^3 in the left lobe in one patient, and 0.31 ml/min/cm^3 in the right lobe and 0.44 ml/min/cm^3 in the left lobe in the other patient.

Liver functional imaging

Liver functional images provided visual display of both anatomical and functional information. As chronic liver disease progressed, a change in liver shape was observed: hypertrophy of the left and/or caudate lobe and atrophy of the right lobe. The K_u was homogeneous in the liver parenchyma in the controls (Fig. 3a). On the other hand, the K_u was reduced and its distribution became more irregular with progression of the underlying liver disease in the patient group. In patients with severe liver profiles (Grade C), hypertrophy of the caudate lobe and a higher K_u in the caudate lobe were demonstrated compared with other liver parenchyma (Fig. 3b). In 2 patients with Budd-Chiari syndrome, the functional images showed hypertrophy of the left lobe and atrophy of the right lobe and clearly demonstrated higher K_u in the left lobe than in the right lobe (Fig. 3c and d).

DISCUSSION

Scatter and attenuation compensation

Scatter and nonuniform attenuation in the body are the most important factors degrading the accuracy of counts toward the interior of the organ in SPECT images of the liver. The usefulness of a TEW scatter and attenuation compensation technique for dynamic studies with Tc-99m sheet line source transmission data has been reported.[14,18–20] We have already reported the accuracy and reliability of this method in a phantom study.[14] SPECT images of a cylindrical water pool phantom containing seven hot rods filled with different concentrations of Tc-99m activity were obtained. The radioactivity measured by SPECT showed good linearity and accuracy with the true radioactivity.

Clinical utility of the proposed method

For quantitative analysis of Tc-99m GSA scintigraphy, non-linear compartment models for GSA receptor binding have been advocated.[6,28] Although good results were reported, they are too troublesome to use in routine studies. Recently, several investigators analyzed Tc-99m GSA scintigraphy with a linear compartment model as in our study and reported good results almost the same as those obtained with a non-linear compartment model. Shinohara et al. have reported that the binding rate constant (K_u) derived from the Patlak plot represents the maximum removal rate of Tc-99m GSA measured in the non-linear compartment model.[17] Hwang measured GSA clearance in the Patlak plot by dynamic SPECT and reported that it strongly reflects hepatic receptor function, but does not show a significant correlation with effective hepatic blood flow.[9] In the present study, we measured the binding rate constant (K_u) at an early stage of several minutes after the injection of Tc-99m GSA. At this early stage, the reverse binding rate constant is considered to be negligibly small compared with the forward binding rate constant. K_u is therefore considered to reflect mainly the forward binding rate constant.[14] Our results showed that measurement of the quantitative K_u value is clinically useful in evaluating liver function. Both total and mean K_u values clearly reflected the severity of chronic liver disease and were significantly correlated with conventional liver function tests and the histological severity of chronic liver disease. The mean K_u value was similar all 5 controls. Although the total K_u values varied since the liver mass needed to meet metabolic requirements depend on body size, the mean K_u was considered to be constant in the absence of inflammation or fibrosis in the liver parenchyma. As periportal necrosis of hepatocytes, intralobular necrosis, portal inflammation and fibrosis progress, the mean K_u value decreases, resulting in a decrease in the total K_u value. These findings confirm the reliability of our method and support the intact hepatocyte theory.[29–31]

Regional liver function

The present method makes it possible to evaluate regional liver function quantitatively. Evaluation of regional liver function provides useful information in patients with many types of liver disease. In patients with Budd-Chiari syndrome, the mean K_u value in the left lobe, where the draining veins were patent was similar to that in the controls, but that in the right lobe, where draining veins were occluded, was reduced. It is known from histological studies that the degree of liver congestion, fibrosis and liver cell necrosis differs depending on the site of hepatic vein occlusion in Budd-Chiari syndrome.[32,33] It was thought that fibrosis and congestion were severe in the right lobes but that histological changes were minimal in the left lobe. Measurement of regional liver function will also be useful in surgical planning. Estimation of remnant liver function is very important in patients with liver tumors who are scheduled to undergo hepatectomy. It may be possible to predict remnant liver function by measuring the K_u of the remnant liver. If we can determine the minimum value for K_u needed to meet metabolic requirements, the K_u value for the remnant liver will be a useful index for determining the degree of surgical intervention.

Liver functional image

Liver functional images clearly reflected the results of total and mean K_u measurements and made it possible to visually assess the severity of chronic liver disease and regional dysfunction of the liver parenchyma. These functional images provided both anatomical and functional information. In patients with chronic liver disease, functional images depicted changes in liver shape and differences in the regional K_u in the liver parenchyma. In patients with severe liver dysfunction, hypertrophy of the caudate lobe and higher K_u in the caudate lobe were demonstrated. In the 2 patients with Budd-Chiari syndrome, functional images demonstrated hypertrophy of the left lobe, and atrophy of the right lobe, and differences in K_u between the right and left lobes. Functional images seems be useful in evaluating the pathophysiology and severity of chronic liver disease. Both anatomical and functional information provided by functional images will be of great value in monitoring regeneration of the remnant liver after hepatectomy, in evaluating transplanted livers, and in following the clinical course after interventional radiology procedures (PTA or transcatheter hepatic arterial chemoembolization).

CONCLUSIONS

In conclusion, receptor imaging with Tc-99m GSA by means of Patlak plot and dynamic SPECT makes it possible to observe total and regional hepatic functional parameters *in vivo*. These data can be obtained qualitatively by attenuation and scatter compensation. Our results suggest that the proposed technique provides unique and diagnostic information that is not available with any other method.

REFERENCES

1. Morell AG, Irvine RA, Sternlieb I, Scheinberg IH, Ashwell G. Physical and chemical studies on ceruloplasmin. V. Metabolic studies on sialic acid-free ceruloplasmin *in vivo*. *J Biol Chem* 1968; 243: 155–159.
2. Aschwell G, Steer CJ. Hepatic recognition and catabolism of serum glycoproteins. *JAMA* 1981; 246: 2358–2364.
3. Stockert RJ, Morell AG. Hepatic binding protein. The galactose-specific receptor of mammalian hepatocytes. *Hepatology* 1983; 3: 750–757.
4. Krohn KA, Vera DR, Stadalnik RC. A complementary radiopharmaceutical model for quantitating hepatic-binding protein receptors. In *Receptor-Binding Radiotracers II*, Eckelman WC, Colombetti LG (eds), Boca Raton; CRC Press, 1982; 41–59.
5. Vera DR, Krohn KA, Stadalnik RC, Scheibe PO. Tc-99m-galactosyl-neoglycoalbumin: *In vivo* characterization of receptor-mediated binding to hepatocytes. *Radiology* 1984; 151: 191–196.
6. Vera DR, Stadalnik RC, Trudeau WL, Scheibe PO, Krohn KA. Measurement of receptor concentration and forward-binding rate constant via radiopharmacokinetic modeling of technetium-99m-galactosyl-neoglycoalbumin. *J Nucl Med* 1991; 32: 1169–1176.
7. Kudo M. Asialoglycoprotein. *Kan tan sui* 1994; 29: 673–681.
8. Stadalnik RC, Vera DR, Krohn KA. Receptor-binding radiopharmaceuticals: Experimental and clinical aspects. In *Nuclear Medicine Annual 1986*, Freeman LM, Weissmann HS (eds), New York; Raven Press, 1986: 105–139.
9. Hwang EH. ^{99m}Tc-GSA dynamic SPECT for mean hepatic functional reserve estimation: assessment of quantification. *KAKU IGAKU (Jpn J Nucl Med)* 1999; 36: 315–322.
10. Fujimori K, Shounai T, Koito K, Yoshida S, Takeda M, Yama N, et al. Estimation of ^{99m}Tc-GSA receptor amount by non-linear 3-compartment model: ligand-receptor binding model without blood sampling. *KAKU IGAKU (Jpn J Nucl Med)* 1999; 36: 753–760.
11. Kudo M, Todo A, Ikekubo K, Hino M. Receptor index via hepatic asialoglycoprotein receptor imaging: correlation with chronic hepatocellular damage. *Am J Gastroenterol* 1992; 87: 865–870.
12. Kawa SHK, Tanaka Y. A quantitative model of technetium-99m-DTPA-galactosyl-HSA for assessment of hepatic binding protein. *J Nucl Med* 1991; 32: 2233–2240.
13. Shuke N, Aburano T, Nakajima K, Yokoyama K, Sun BF, Matsuda H, et al. The utility of quantitative ^{99m}Tc-GSA liver scintigraphy in the evaluation of hepatic functional reserve: comparison with ^{99m}Tc-PMT and ^{99m}Tc-Sn colloid. *KAKU IGAKU (Jpn J Nucl Med)* 1991; 29: 573–584.
14. Ichihara T, Maeda H, Yamakado K, Motomura N, Matsumura K, Takeda K, et al. Quantitative analysis of scatter- and attenuation-compensated dynamic single-photon emission tomography for functional hepatic imaging with a receptor-binding radiopharmaceutical. *Eur J Nucl Med* 1997; 24: 59–67.
15. Rutland MD. A single injection technique for subtraction of blood background in I-131-hippuran renograms. *Br J Radiol* 1979; 52: 134–137.
16. Patlak CS, Blasberg RG, Fenstermacher JD. Graphical evaluation of blood-to-brain transfer constants from multiple-time uptake data. *J Cereb Blood Flow Metab* 1983; 3: 1–7.
17. Shinohara H, Niio Y, Hasebe S, Matsuoka S, Obuchi M, Higashi TS, et al. Quantitative analysis of ^{99m}Tc-GSA liver scintigraphy with graphical plot method. *Nippon Igaku Hoshasen Gakkai Zasshi* 1996; 56 (4): 208–214.
18. Ichihara T, Ogawa K, Motomura N, Kubo A, Hashimoto S. Compton-scatter compensation using the triple energy window method for single and dual isotope SPECT. *J Nucl Med* 1993; 34: 2216–2221.
19. Ichihara T, Motomura N, Hasegawa H, Ogawa K, Hashimoto J, Kubo A. Improved transmission tomography using flood source and TEW scatter correction for attenuation compensation. *J Nucl Med* 1995; 36: 166.
20. Hashimoto J, Sammiya T, Ogasawara K, Kubo A, Ogawa K, Ichihara T, et al. Scatter and attenuation correction for quantitative myocardial SPECT using transmission measurement with a sheet line source. *KAKU IGAKU (Jpn J Nucl Med)* 1996; 33: 1015–1019.
21. Ogawa K, Takagi Y, Kubo A, Hashimoto S, Sanmiya T, Okano Y, et al. An attenuation correction method of single

photon emission computed tomography using gamma ray transmission CT. *Jpn J Nucl Med* 1985; 22: 477–490.
22. Yamanaka N, Okamoto E, Kawamura E, Kato T, Oriyama T, Fujimoto J, et al. Dynamics of normal and injured liver regeneration after hepatectomy as assessed on the basis of computed tomography and liver function. *Hepatology* 1993; 18: 79–85.
23. Chen M, Hwang T, Hung C. Human liver regeneration after major hepatectomy. A study of liver volume by computed tomography. *Ann Surg* 1991; 213: 227–229.
24. Shimada M, Matsumata T, Maeda T, Itasaka H, Suehiro T, Sugimachi K. Hepatic regeneration following right lobectomy: estimation of regenerative capacity. *Surg Today* 1994; 24: 44–48.
25. Zeman RK, Fox SH, Silverman PM, Davros WJ, Carter LM, Griego D, et al. Helical (spiral) CT of the abdomen. *AJR* 1993; 160: 719–725.
26. Pugh RN, Murray-Lyon IM, Dawson JL, Pietroni MC, Williams R. Transection of the oesophagus for bleeding oesophageal varices. *Br J Surg* 1973; 60: 646–649.
27. Knodell RG, Ishak KG, Black WC, Chen TS, Craig R, Kaplowitz N, et al. Formulation and application of a numerical scoring system for assessing histological activity in asymptomatic chronic active hepatitis. *Hepatology* 1981; 5: 431–435.
28. Ha-Kawa SK, Tanaka Y. A quantitative model of technetium-99m-DTPA-galactosyl-HSA for the assessment of hepatic blood flow and hepatic binding receptor. *J Nucl Med* 1991; 32: 2233–2240.
29. Wood AJJ, Villeneuve JP, Branch RA, Rogers LW, Shand DJ. Intact hepatocyte theory of impaired drug metabolism in experimental cirrhosis in the rat. *Gastroenterology* 1979; 76: 1358–1362.
30. Gartner U, Stockert RJ, Morell AG, Wolkoff AW. Modulation of the transport of bilirubin and asialoorosomucoid during liver regeneration. *Hepatology* 1981; 1: 99–106.
31. Kawasaki S, Imamura H, Bandai Y, Sanjo K, Idezuki Y. Direct evidence for intact hepatocyte theory in cirrhotic patients. *Gastroenterology* 1991; 100: A759.
32. Murphy FB, McDermott WV, Sone MD, Bothe A, Trey C. Budd-Chiari syndrome: historical and clinical review with analysis of surgical corrective procedures. *Am J Surg* 1984; 147: 463–467.
33. Lisbona R, Katz S, Mishkin S. Serial radionuclide liver imaging in Budd-Chiari syndrome. *J Can Assoc Radiol* 1981; 32: 175–177.